International Journal for Housing Science and Its Applications
Publish August 4, 2025. Volume 46, Issue 3 Pages 2087-2101

https://doi.org/10.70517/ijhsa463165

Meta-heuristic algorithm-based power structure management and transition path planning under the implementation of dual-carbon strategy

Jingui Zhang[1,*] and Zhonghua Li[2]
[1] MBA Center, Shandong University of Technology, Zibo, Shandong, 255000, China
[2] School of Marxism, Shandong University of Technology, Zibo, Shandong, 255000, China
Corresponding authors: (e-mail: zjg_bz@163.com).

Abstract Under the background of “dual-carbon” strategy, this paper proposes a path planning method for low-carbon transition of power system integrating dynamic carbon oriented mechanism and meta-heuristic algorithm. By constructing a dual low-carbon demand response model and a stepped carbon trading model, and combining with the refined simulation framework of EnergyPLAN platform, a multi-objective optimization model is established from the three dimensions of power supply, carbon emission and costing. Parameter planning and Nash negotiation game theory are introduced to generate the Pareto frontier equilibrium solution, and the cooperative scheduling optimization of microgrid cluster is realized based on CPLEX tool. The simulation results show that microgrids A and B realize the improvement of power flow efficiency within the system through the time-sharing tariff mechanism (peak tariff of 0.82 yuan/kWh and low valley tariff of 0.25 yuan/kWh), and the internal tariff is 12%-18% lower than that of the external grid, which promotes the consumption of renewable energy. The total power generation costs under low, medium and high risk scenarios are 47.68 trillion, 53.12 trillion and 58.45 trillion yuan respectively, and carbon emissions are reduced to 2,444.33Mt, 2,142.21Mt and 1,793.55Mt respectively at the end of the planning period, and the average annual emission reduction under the high-risk scenario reaches 648.84Mt, which improves the emission reduction efficiency by 37% compared with that of the low carbon price scenario. The sensitivity analysis shows that when the carbon price is raised from 30 yuan/ton to 100 yuan/ton, the medium-risk scenario reduces carbon emissions by 237 million tons, and the total cost is reduced by 0.81 trillion yuan. When the share of energy storage is increased from 5% to 15%, the unit generation cost of the high-risk scenario decreases by 0.039 yuan/kWh, saving 2.07 trillion yuan.

Index Terms meta-heuristic algorithms, low-carbon transition pathways, EnergyPLAN, Pareto frontier equilibrium solution, electricity supply, carbon emissions

I. Introduction

In the past decade, China's economy has realized double-digit annual growth and is the second largest economy in the world, and the rapid economic development has also brought great challenges to resources and the environment. Currently, China is the world's largest coal producing and consuming country, and also the world's largest carbon emitting country, the requirement of clean and low carbon energy transition is very urgent [1], [2]. Against the background of global climate change and energy transition, China has put forward a “double carbon” strategic goal, i.e., to achieve carbon peak by 2030 and carbon neutrality by 2060. The power industry is a pillar industry of the national economy that has a bearing on the national economy and people's livelihood, and it is also the sector with the largest carbon emissions in China. Energy combustion accounts for about 88% of all carbon dioxide emissions, and emissions from the power industry account for about 41% of the total, so the power industry itself has a difficult task of carbon emission reduction [3]-[5]. At the same time, the clean-up of the power industry will help upgrade the energy consumption pattern of the whole society and support the key energy-consuming industries such as iron and steel, chemical industry and building materials to improve the efficiency of energy utilization [6], [7]. Therefore, the electric power industry is an important field for carbon emission reduction and a main battlefield for realizing the “dual-carbon” strategy. The core of China's “dual-carbon” strategy is to continuously increase the proportion of non-fossil energy consumption, mainly through electrification [8]. In order to realize this strategic goal, the structural transformation of the power system has become crucial. In addition, more than 90% of non-fossil energy must be converted into electricity to be utilized to regulate carbon emissions, and 80% of the future incremental non-fossil energy is new energy power generation mainly based on wind and light, while new energy has the characteristics of random fluctuation of output, low disturbance and weak support, which is still very

different from that of the power grid constructed with traditional synchronous generators [9], [10]. Therefore, in order to adapt to the very high proportion of new energy access and consumption, China's power system must be revolutionized and upgraded.

Currently, China's power system is committed to promoting the transformation of the power structure from high-carbon to low-carbon and from fossil energy-based to clean energy-based, accelerating the construction of a new type of power system with a gradual increase in the proportion of new energy sources, and the optimization of the power structure has brought about the continuous optimization of the power industry's carbon emission reduction intensity index [11]-[13]. However, power structure optimization under multiple constraints, the penetration rate of renewable energy and the frequency deviation of the power system is difficult to balance, and the penetration rate exceeds a certain threshold, and the frequency deviation increases. At the same time, energy deployment and regional power resource allocation are unreasonable, leading to energy waste, and the flexibility of energy resource dispatch constrains the peak demand of the power system, all of which affect the stability, economy, security, and power supply quality of the power system [14]-[16]. Meta-heuristic algorithms are methods that enable the search for optimal solutions from a given space in a spontaneous, efficient, and flexible manner. It can be defined as a way to go beyond a single, visual optimization approach for solving combinatorial optimization problems with high suitability in solving problems such as power structure optimization, path planning, and capacity allocation [17].

This paper focuses on the analysis of power system low-carbon mechanism, the construction of power sector model and multi-objective optimization algorithm, and puts forward a set of methodology system integrating the dynamic carbon oriented mechanism and engineering game theory, which provides theoretical support and practical path for the low-carbon transformation of power system. Firstly, in the analysis of low-carbon mechanism of power system, the linkage mechanism between user behavior and carbon market is constructed through the “dual low-carbon demand response model” and “ladder-type carbon trading model”. Among them, the price-based demand response based on dynamic carbon emission factors guides users' energy use behavior through time-sharing tariffs, while the incentive-based demand response driven by nodal carbon potentials combines with the transferable/reducible load model to realize low-carbon scheduling in the spatial and temporal dimensions. Meanwhile, the ladder-type carbon trading model further strengthens users' initiative to participate in carbon reduction through carbon emission right trading and dynamic adjustment of carbon cost. On this basis, the EnergyPLAN model is used as the core, and a refined simulation framework is constructed from the three dimensions of power supply, carbon emission and costing respectively. The power sector module quantifies the difference between renewable energy and thermal power generation through correction factors and hourly distribution, the carbon emission module combines fuel consumption and carbon emission factors to realize system-wide carbon accounting, and the cost module provides economic constraints for the optimization algorithm through the multi-dimensional analysis of investment, operation and maintenance, fuel and carbon costs. The multi-objective optimization algorithm proposes a Pareto frontier solution based on parameter planning and an engineering game optimization method for the synergistic goal of wind power consumption and carbon emission reduction. The former transforms the multi-objective problem into single-objective optimization through the constraint method, and generates the Pareto frontier by combining the division of key areas, while the latter introduces the Nash negotiation game theory, and reaches the equilibrium solution through the negotiation of the virtual participants, which solves the decision-making optimization problem under the multi-objective conflict.

II. Power system low carbon mechanism analysis and multi-objective optimization model construction

II. A. Analysis of Low Carbon Mechanisms in Power Systems

II. A. 1) Dual low-carbon demand response modeling

(1) Price-based low-carbon demand response based on dynamic carbon emission factors

In this paper, we attach carbon orientation to time-of-day tariffs, use dynamic carbon emission factors to distinguish peak and valley periods of tariffs, and divide them into high-carbon, medium-carbon, and low-carbon electricity consumption periods, raise tariffs in high-carbon emission periods, lower tariffs in low-carbon emission periods, and keep tariffs stable in medium-carbon emission periods. The carbon-oriented tariffs guide users to increase electricity consumption during low-carbon emission periods and decrease electricity consumption during high-carbon emission periods, thus promoting changes in users' energy consumption behaviors and realizing user-driven carbon emission reduction goals of the power system.

The fuzzy affiliation function is used to analyze the carbon emission period based on the dynamic carbon emission factor, and the model is as follows.

$$\begin{cases} \mu_1\left(\varepsilon_t^j\right)=\dfrac{\varepsilon_t^j-\varepsilon^{\min}}{\varepsilon^{\max}-\varepsilon^{\min}} \\ \mu_2\left(\varepsilon_t^j\right)=\dfrac{\varepsilon^{\max}-\varepsilon_t^j}{\varepsilon^{\max}-\varepsilon^{\min}} \end{cases} \tag{1}$$

where: $\varepsilon^{\min}$, $\varepsilon^{\max}$ are the minimum and maximum values of the dynamic carbon emission factor, respectively.

The peak and valley affiliation of the maximum value point on the dynamic carbon emission factor curve is 1, 0, and the minimum value point is 0, 1, respectively, and the affiliation threshold is set as $\lambda_1,\lambda_2\in(0,1)$. The time period with $\mu_1(\varepsilon_t^j)>\lambda_1$ is classified as high carbon time period, the time period with $\mu_2(\varepsilon_t^j)<\lambda_2$ is classified as low carbon time period, and the rest is classified as medium carbon time period.

The electricity price elasticity matrix method is selected to model the demand response, and its mathematical model is

$$m=\frac{\Delta L_e/L_e}{\Delta c_p/c_p} \tag{2}$$

where: m is the electricity tariff elasticity index; L_e, ΔL_e are the electricity quantity and its change, respectively; c_p, Δc_p are the electricity price and its change, respectively.

(2) Incentive-based low-carbon demand response based on nodal carbon potentials

This paper utilizes the nodal carbon potential as an incentive signal and introduces a carbon reward and penalty mechanism. Users adjust their energy use behavior according to the carbon potential, and the dispatchable loads considered in this paper include transferable loads and curtailable loads. Based on the proposed carbon reward and penalty incentive mechanism, the transferable load will be transferred from the node with higher carbon potential to the node with lower carbon potential, and the curtailable load will be curtailed in the node with higher carbon potential, so as to realize low-carbon dispatch in both time and space dimensions, and thus achieve the purpose of eliminating the wind and reducing the carbon emission of the system.

The transferable load model is established as

$$\begin{cases} C_{shift,t}=C_{shift,t}^{dis}+C_{shift,t}^{re} \\ C_{shift,t}^{dis}=K_{shift}^{dis}\left(P_{shift,t}^{tra,in}+P_{shift,t}^{tra,out}\right) \end{cases} \tag{3}$$

$$C_{shift,t}^{re}=\begin{cases} K_{shift,1}^{re}\left(P_{shift,t}^{tra,in}-P_{shift,t}^{tra,out}\right), e_{\min}\le e_{i,t}\le\dfrac{1}{2}\left(e_{\max}+e_{ave}\right) \\ K_{shift,2}^{re}\left(P_{shift,t}^{tra,in}-P_{shift,t}^{tra,out}\right), \dfrac{1}{2}\left(e_{\max}+e_{ave}\right)\le e_{i,t}\le\dfrac{1}{2}\left(e_{\max}+e_{ave}\right) \\ K_{shift,3}^{re}\left(P_{shift,t}^{tra,in}-P_{shift,t}^{tra,out}\right), \dfrac{1}{2}\left(e_{\max}+e_{ave}\right)\le e_{i,t}\le_{\max} \end{cases} \tag{4}$$

where: $C_{shift,t}$ is the total dispatch cost of transferable load; $C_{shift,t}^{dis}$ is the base dispatch cost; $C_{shift,t}^{re}$ is the incentive-based low-carbon demand response carbon bonus and penalty cost; K_{shift}^{dis} is the unit dispatch cost of transferable load; $K_{shift,1}^{re}$, $K_{shift,2}^{re}$, $K_{shift,3}^{re}$ are the unit carbon penalty costs of the transferable loads at different node carbon potentials; $P_{shift,t}^{tra,in}$, $P_{shift,t}^{tra,out}$ are the amount of transferable loads transferring into and out of the load at the moment t, respectively; $e_{\min}$, $e_{\max}$, and e_{ave} are the minimum, maximum, and average values of the carbon potential of the load node at moment t, respectively.

The model of curtailable load is established as

$$\begin{cases} C_{cut,t}=C_{cut,t}^{dis}+C_{cut,t}^{re} \\ C_{cut,t}^{dis}=K_{cut}^{dis}P_{cut,t} \end{cases} \tag{5}$$

$$C_{cut,t}^{re}=\begin{cases} K_{cut,1}^{re}P_{cut,t}, e_{\min}\le e_{i,t}\le\dfrac{1}{2}\left(e_{\min}+e_{ave}\right) \\ K_{cut,2}^{re}P_{cut,t}, \dfrac{1}{2}\left(e_{\min}+e_{ave}\right)\le e_{i,t}\le\dfrac{1}{2}\left(e_{\max}+e_{ave}\right) \\ K_{cut,3}^{re}P_{cut,t}, \dfrac{1}{2}\left(e_{\min}+e_{ave}\right)\le e_{i,t}\le e_{\max} \end{cases} \tag{6}$$

where: $C_{cup,t}$ is the total dispatch cost of the load that can be curtailed; $C_{cut,t}^{dis}$ is the base dispatch cost; $C_{cut,t}^{re}$ is the incentive-based low-carbon demand response carbon reward and penalty cost; $P_{cut,t}$ is the amount of load that can be cut at moment t.

II. A. 2) Stepped carbon trading model based on nodal carbon potentials

This paper establishes a step carbon emissions trading model based on nodal carbon potential, which is used to improve the initiative of users to participate in energy saving and carbon reduction in the power system. The system load participates in the carbon emissions trading market to realize the effective trading of carbon emission rights, and its actual carbon emission rights trading amount D^{tr} is

$$D^{tr} = D^{ac} - D^{q} \tag{7}$$

where: D^{ac} is the actual carbon emissions of the system load during the dispatch period; D^{q} is the initial carbon emission quota obtained by the system load in the carbon trading market.

$$D^{ac} = \sum_{t=1}^{T} e_{i,t} \left(P_t^{PDR} + P_{shift,t}^{tra,in} - P_{shift,t}^{tra,out} - P_{cut,t} \right) \Delta t \tag{8}$$

where: P_t^{PDR} is the load after price-based demand response at moment t.

The stepped carbon transaction cost is expressed as

$$C_L^{co} = \begin{cases} \lambda D^{tr} & D^{tr}, d \\ \lambda(1+\alpha)(D^{tr}-d)+\lambda d & d < D^{tr}, 2d \\ \lambda(1+2\alpha)(D^{tr}-2d)+\lambda(2+\alpha)d & 2d < D^{tr}, 3d \\ \lambda(1+3\alpha)(D^{tr}-3d)+\lambda(3+3\alpha)d & 3d < D^{tr}, 4d \\ \lambda(1+4\alpha)(D^{tr}-4d)+\lambda(4+6\alpha)d & D^{tr} > 4d \end{cases} \tag{9}$$

where: D^{tr} is the actual carbon emissions trading amount; λ is the carbon trading benchmark price; d is the length of the carbon emissions interval; and α is the price growth factor.

II. B.Power sector modeling

Based on the above low-carbon mechanism analysis, the realization of the carbon reduction target of the power system needs to rely on accurate model construction and simulation. To this end, this section further combines the EnergyPLAN platform to construct a refined model from the three dimensions of power supply, carbon emission and costing to provide data support and constraints for subsequent optimization.

II. B. 1) Electricity sector module

The main inputs to the power sector module of the EnergyPLAN model are the total power demand, total power supply and outgoing and imported power for the simulation year. In particular, the electricity supply from renewable energy generation technologies such as photovoltaic, wind, hydroelectric, and nuclear is obtained by multiplying the corresponding capacity by a specified hourly distribution. It should be noted that since differences in the configuration of renewable power generation units can lead to different power production in different years at the same capacity, the EnergyPLAN model is set with corresponding trimming factors to reflect the different production by changing the distribution. The power generation calculations for renewable energy generation technologies such as photovoltaic, wind, hydropower and nuclear power technologies are shown in Eqs. (10)-(17):

$$S_{Ele,Hydro} = \eta_{hydro} \sum_{t=1}^{N_{year}} C_{hydro}^{Ins} \times l_{Ele,hydro,dis}(t) \tag{10}$$

$$S_{Ele,wind} = \eta_{wind} \sum_{t=1}^{N_{year}} C_{wind}^{Ins} \times l_{Ele,wind,dis}(t) \tag{11}$$

$$S_{Ele,PV} = \eta_{PV} \sum_{t=1}^{N_{year}} C_{PV}^{Ins} \times l_{Ele,PV,dis}(t) \tag{12}$$

$$S_{Ele,Geo} = \eta_{Geo} \sum_{t=1}^{N_{year}} C_{Geo}^{Ins} \times l_{Ele,Geo,dis}(t) \tag{13}$$

$$S_{Ele,Nuclear} = \eta_{Nuclear} \sum_{t=1}^{N_{year}} C_{Nuclear}^{Ins} \times l_{Ele,Nuclear,dis}(t) \tag{14}$$

where $S_{Ele,Hydro}$, $S_{Ele,wind}$, $S_{Ele,PV}$, $S_{Ele,Geo}$, $S_{Ele,nuclear}$ are the electricity generation from hydroelectricity, wind power, photovoltaic, geothermal and nuclear energy, respectively, $l_{Ele,Hydro,dis}(t)$, $l_{Ele,wind,dis}(t)$, $l_{Ele,PV,dis}(t)$, $l_{Ele,Geo,dis}(t)$, and $l_{Ele,nuclear,dis}(t)$ are the hourly distributions of the above generation categories, and the hourly distributions of the above generation categories are the hourly distributions of the above generation categories. Hourly distributions of the above power generation categories will be directly input into the model with data normalization; η_{hydro}, η_{wind}, η_{PV}, η_{Geo}, $\eta_{nuclear}$ are the correction factors for hydroelectricity, wind power, photovoltaic, geothermal and nuclear energy generation respectively; C_{hydro}^{Ins}, C_{wind}^{Ins}, C_{PV}^{Ins}, C_{Geo}^{Ins}, and $C_{nuclear}^{Ins}$ are the installed capacity of hydroelectricity, wind power, photovoltaic power, geothermal energy, and nuclear energy generation, respectively; N_{year} is the total number of annual hours, which is set to 8784 in this chapter.

The operation logic of the thermal power unit module in the Energy PLAN model is set to have a low generation priority for this technology, and when its generation $S_{Ele,PP}(t)$ is less than the total installed capacity of the thermal power plant C_T^{Ins} in the t moment, the value of its power generation is determined as the difference between the total electric power demand and the generation from other power sources, and when there are generating units of different fuels in the thermal power, its specific calculation is shown in equations (15)-(17):

$$C_T^{Ins} = C_{T,coal}^{Ins} + C_{T,Ngas}^{Ins} + C_{T,bio}^{Ins} \tag{15}$$

$$\begin{cases} s_{Ele,PP}(t) = d_{Ele}(t) - s_{Ele,1}(t) & d_{Ele}(t) - s_{Ele,1}(t) < C_T^{Ins} \\ s_{Ele,PP}(t) = C_T^{Ins} & d_{Ele}(t) - s_{Ele,1}(t) > C_T^{Ins} \end{cases} \tag{16}$$

$$S_{Ele,PP} = \sum_{t=1}^{N_{year}} s_{Ele,PP}(t) \tag{17}$$

where C_T^{Ins}, $C_{T,coal}^{Ins}$, $C_{T,Ngas}^{Ins}$, $C_{T,bio}^{Ins}$ are the total installed capacity of thermal power, installed capacity of coal-fired units, installed capacity of gas-fired units, installed capacity of biomass-fueled thermal power units, respectively; $s_{Ele,PP}(t)$, $d_{Ele}(t)$, and $s_{Ele,1}(t)$ are the power generation capacity of thermal power units, the total demand for electricity, and the demand for other power generation technologies at the moment of t, respectively, and $S_{Ele,PP}$ is the power generation capacity of thermal power.

The energy storage technology module in the Energy PLAN model consists of a charging device, a discharging device and a storage capacity. The charging device converts electrical energy into potential energy and the discharging device converts potential energy into electrical energy, both defined by its installed capacity C_{charge}^{Ins} and $C_{discharge}^{Ins}$; the storage capacity represents the ability to store energy, defined by the energy storage $E_{storage}^{Ins}$. The energy storage operating equation is shown in (18):

$$s_{Ele,sto}(t) = \begin{cases} \dfrac{s_{Ele,in}(t)}{\eta_{ch}} & s_{Ele,in}(t) > 0 \\ \eta_{dis} s_{Ele,in}(t) & s_{Ele,in}(t) < 0 \end{cases} \tag{18}$$

In the formula, $s_{Ele,sto}(t)$, $s_{Ele,in}(t)$ are t moment energy storage internal input power, the system outside the input power, $s_{Ele,in}(t)$ is positive on behalf of the energy storage in the charging state, $s_{Ele,in}(t)$ is positive on behalf of the energy storage in the discharging state; η_{ch}, η_{dis} are the energy storage charging and discharging efficiencies, respectively. During system operation, the energy storage model follows the installed capacity power constraint, storage capacity constraint, and total charging and discharging constraints, which are not further described here.

II. B. 2) Carbon Emissions Module

The CO_2 emissions in the Energy PLAN model are defined as generated by the energy combustion process, so CO_2 emissions are calculated by the energy carbon emission factor with the energy consumption as shown in Equation (19):

$$E_{CO_2} = \sum_i e_{CO_2}(i) = \sum_j s_j \times \delta_j = \sum_i \sum_j s_{ij} \times \delta_j \tag{19}$$

where E_{CO_2} denotes the total system CO2 emissions, i refers to the end-use sector, j refers to the fuel type, $e_{CO_2}(i)$ refers to the CO2 consumption in that sector, s_j denotes the consumption of a certain fuel, δ_j denotes the CO_2 emission factor of that fuel, s_{ij} denotes the consumption of j fuel in i sector.

II. B. 3) Cost module

Energy PLAN simulates systems on a yearly basis, so its cost module also outputs technology investment costs, fixed and variable O&M costs, fuel costs, and carbon emission costs on a yearly basis. First, the annual cost of each technology will be calculated, including the technology investment cost and fixed O&M cost and variable O&M cost. The annual investment cost is mainly determined by inputs such as technology capacity, technology unit cost, lifetime, discount rate, etc., which are calculated as follows:

$$\begin{aligned} T_{yinv} &= \sum_i T_{yinv,i} = \sum_i T_{inv,i} \times \frac{m}{1-(1+m)^{-n_i}} \\ &= \sum_i C_i^{Ins} \times P_i^{unit} \times \frac{m}{1-(1+m)^{-n_i}} \end{aligned} \tag{20}$$

where i refers to the specific technology, $T_{yinv,i}$, $T_{inv,i}$ are the annual cost and total investment cost of the i th technology, C_i^{Ins}, P_i^{unit} are the i th technology and the unit investment cost, respectively; n_i is the expected life of the i th technology, and m is the discount rate.

The formula for the annual fixed O&M cost is as follows:

$$T_{yOM} = \sum_i T_{yOM,i} = \sum_i p_{yOM,i} \times T_{inv,i} \tag{21}$$

where i refers to the specific technology, $T_{yOM,i}$ and $T_{inv,i}$ are the annual fixed O&M cost and the total investment cost of the i th technology, respectively, and $p_{yOM,i}$ is the percentage factor of the annual fixed O&M cost of the i th technology to the investment cost.

The formula for annual variable O&M cost is as follows:

$$T_{yVOM} = \sum_i T_{yVOM,i} = \sum_k \sum_i p_{yVOM,i} \times S_{k,i} \tag{22}$$

where k refers to the terminal sector and i refers to the specific technology; $T_{yVOM,i}$ is the annual variable O&M cost of the i th technology, $S_{k,i}$ is the annual amount of energy supplied to the i th technology, and $p_{yVOM,i}$ is the annual variable O&M cost calculation factor of the i th technology.

The formula for calculating the fuel cost is as follows:

$$T_{yfuel} = \sum_j T_{yfuel,j} = \sum_j p_{fuel,j} \times E_j \tag{23}$$

where j refers to the specific fuel, T_{yfuel} is the total annual fuel cost of the system, $T_{yfuel,j}$ is the annual fuel cost of the j th fuel; $p_{fuel,j}$ is the price of the i th fuel, and E_j is the annual consumption of the j th fuel.

The formula for calculating the cost of carbon emissions is as follows:

$$T_{yCO_2} = p_{CO_2} \times E_{CO_2} \tag{24}$$

where T_{yCO2} is the total annual emission cost of the system, p_{CO2} is the carbon emission cost factor, and E_{CO2} is the annual carbon emission of the system.

II. C.Multi-objective optimization algorithm

After completing the power sector model construction and cost-carbon emission accounting, how to achieve multi-objective co-optimization becomes critical. This section proposes a composite optimization method based on parameter planning and engineering game to solve the complex trade-off between wind power consumption, carbon emission reduction and economy through Pareto frontier solving and virtual participant negotiation mechanism.

II. C. 1) Parameter planning based solution to the Pareto frontier

The problem takes into account the uncertainty and instability of wind power as well as the introduction of energy storage technology, and aims to maximize the utilization and economy of wind power while reducing carbon emissions, which can be modeled as a multi-objective linear optimization problem. As shown in equation (25).

$$\begin{cases} \min(c_1^T x, c_2^T x, c_3^T x) \\ s.t. A_x \le b \end{cases} \tag{25}$$

where: x is the decision variable to be optimized; A, b are the constraints in the problem; c_1, c_2, c_3 are the weights of different objectives.

In a multi-objective optimization problem, it is often desirable to find a set of solutions that are optimal under multiple objective functions. The ε-constraint method is a commonly used method to transform a multi-objective optimization problem into a single-objective optimization problem by introducing ε-constraints. Specifically, a ε value is introduced for each objective function, which constrains the objective function to a ε range. By adjusting the ε value to a range of solutions, these solutions constitute the Pareto frontier. Parameter programming, on the other hand, is a special type of optimization problem in which some of the coefficients in the optimization problem are functions with respect to a set of parameters. This is shown in equation (26).

$$\begin{cases} \min v = c^T x \\ s.t. A_x \le b + B_\theta \end{cases} \tag{26}$$

where: c determines the coefficients of the objective function; B is the coefficients of the constraints; and θ takes values in the domain of definition Θ. The constraints $B_\theta \le \theta$ limit the range of values of the variable x, which can ensure that the solution satisfies the actual constraints of the problem. Solving the problem yields the corresponding optimal solution $x^*(\theta)$ and optimal value $v^*(\theta)$. Different aspects of the problem are investigated by varying the value of θ to understand the optimal solution and optimal value in different cases.

The critical region is a subset of the parameter space Θ which is defined by a specific set of constraints. The ε constraint based method is shown in equation (27).

$$\begin{cases} \min v_1 = c_1^T x \\ s.t. A_x \le b \\ c_2^T x \le \varepsilon_2 \\ c_3^T x \le \varepsilon_3 \end{cases} \tag{27}$$

where: ε_2, ε_3 are regarded as the parameters of the problem, and their values affect the optimal solution and optimal value of the problem, whose parameter space is shown in Equation (28).

$$\Theta = \left\{ (\varepsilon_2, \varepsilon_3) \mid \varepsilon_2^l \le \varepsilon_2 \le \varepsilon_2^u, \varepsilon_3^l \le \varepsilon_3 \le \varepsilon_3^u \right\} \tag{28}$$

where: ε_3^u is the upper bound of ε_3, i.e., the value of ε_3 can not be taken more than ε_3^u; ε_3^l is the lower bound of ε_3 is the lower bound of ε_3, i.e., the value of ε_3 cannot be taken less than ε_3^l. Limit the value of ε_3 to be taken between ε_3^l and ε_3^u.

The optimal solution x^* satisfies Equation (29) when $(\varepsilon_2, \varepsilon_3) \in \Theta$.

$$\begin{aligned} c_2^T x^* &= \varepsilon_2 \\ c_3^T x^* &= \varepsilon_3 \end{aligned} \tag{29}$$

By definition, a solution lies on the Pareto front if it cannot be dominated by any other solution in the objective function space. Thus, $(v_1, \varepsilon_2, \varepsilon_3)$ is a point on the Pareto front. Within each key region, the optimal value v^* is represented by a linear function of a linear combination of the parameters θ. Each hyperplane corresponds to a critical region within the parameter space. These hyperplanes represent optimal solutions at different values of the parameters and form Pareto fronts between them. Different values of the parameters lead to different hyperplanes and thus different optimal solutions. Multiple optimal solutions on the Pareto front are obtained by exploring different regions in the parameter space.

II. C. 2) Engineering game-based multi-objective optimization approach

The Nash Negotiation Game Method is a solution in game theory that utilizes negotiation and cooperation to find an equilibrium between participants. Each subject has its own cost function and wants to achieve the goal of minimizing its own cost through negotiation and cooperation. Consider the multi-objective optimization problem as a negotiation game with three virtual participants. Each virtual participant's negotiation goal is to minimize its own cost function, and through the game and negotiation to reach an agreement and find an equilibrium point. This equilibrium point corresponds to the optimal solution of the multi-objective optimization problem.The topology of the 5-node system is schematically shown in Fig. 1.

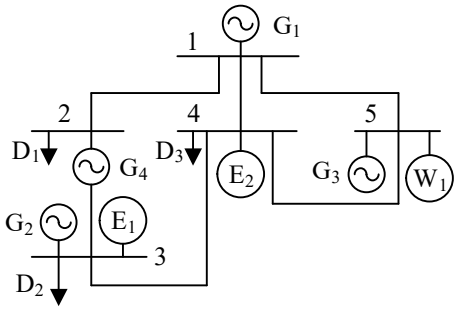

Figure 1: The topological structure diagram of the 5-node system

Equation (30) is shown.

$$\begin{cases} v_1 = c_1^T x \\ v_2 = c_2^T x \\ v_3 = c_3^T x \end{cases} \tag{30}$$

A parameter planning algorithm is used to solve the multi-objective optimization problem. The parameter planning algorithm is an optimization method based on parameter space search, which searches for the optimal solution by adjusting the values of the parameters, as shown in Equation (31).

$$v_1 = p_i v_2 + q_i v_3 + r_i, (v_2, v_3) \in C_{R_i} \tag{31}$$

The analytic expressions for v_1 with respect to (v_2, v_3) in the key regions are obtained by computation. These analytic expressions describe the relationship between v_1 and the other objective variables v_2 and v_3 in each critical region.

In a multi-objective optimization problem, each critical region CR_i is considered as an engineering game problem. An engineering game is a solution in game theory that treats the decision problem as a game problem between multiple participants, as shown in Equation (32).

$$\begin{cases} \max J_i = (p_i \overline{v}_2 + q_i \overline{v}_3 + \overline{r}_i)\overline{v}_2 \overline{v}_3 \\ s.t.(\overline{v}_2, \overline{v}_3) \in \overline{C}_{R_i} \end{cases} \tag{32}$$

Check if the condition $p_i q_i \neq 0$ is satisfied and $\left(\overline{v}_2^*, \overline{v}_3^*\right) \in \overline{C}_{R_i}^*$ is satisfied. If it is satisfied, then $\left(\overline{v}_2^*, \overline{v}_3^*\right)$ is the optimal solution.

If the above condition is not satisfied, it means that the optimal solution is obtained on the boundary of C_{R_i}. In this case, it is necessary to take $\overline{v}_3$ to be an affine function with respect to $\overline{v}_2$. Using this affine function, the problem is transformed into a single objective optimization problem. Solve this single-objective optimization problem to find the optimal solution of $\left(\overline{v}_2^*, \overline{v}_3^*\right)$. This optimal solution corresponds to the optimal decision point on the boundary of CR_i. The computational procedure is shown in Eq. (33).

$$\begin{cases} \overline{v}_2^* = -\dfrac{\overline{r}_i}{3p_i} \\ \overline{v}_3^* = -\dfrac{\overline{r}_i}{3q_i} \end{cases} \tag{33}$$

Calculate the optimal values J_i for the engineering game problem corresponding to each critical region CR_i. These optimal values describe the optimal decision scheme within each critical region. The largest optimal value J^* is identified from these optimal values and its corresponding objective value (v_1^*, v_2^*, v_3^*) is determined. This objective value is the final decision point, which represents the optimal solution in a multi-objective optimization problem.

III. Validation of microgrid modeling and multi-objective co-optimization based on meta-heuristic algorithm

After completing the analysis of the low-carbon mechanism of power system and the theoretical construction of the multi-objective optimization model, this chapter focuses on the practice of microgrid system under the dual-carbon

strategy, combines the EnergyPLAN platform with the improved snake optimization algorithm to design the multi-microgrid cooperative scheduling model, and verifies the practical effect of the dynamic carbon-directed mechanism and the game optimization method through simulation.

III. A. Solution approach

In this paper, three microgrids are designed, and the parameter design of each microgrid is specifically shown in Table 1, on the basis of which the EnergyPLAN system is established.

Table 1: Parameter design of each microgrid

Power supply type	Microgrid			Set		Operation and maintenance cost coefficient / (Yuan /kWh)
	A	B	C	Upper limit /kW	Lower limit /kW	
Wind turbine	1	1	1	200	0	0.0374
Photovoltaic unit	1	1	2	150	0	0.088
Battery	1	0	1	100	-100	0.0011
Gas turbine	1	1	1	100	0	0.0452
Fuel engine	1	1	1	100	0	0.0813

To verify the validity of the experiments, the microgrid model EnergyPLAN modeling is carried out using CPLEX tool in the environment of Matlab 2018b. The outer layer of this paper utilizes the improved snake optimization algorithm for pricing as well as setting of various optimization parameters. The inner layer utilizes the solver to optimize the upper EnergyPLAN model and the lower microgrid cluster model respectively. In the simulation, a 600 kWh battery is selected, the initial state of charge is 200 kWh, the maximum power for the energy storage included in EnergyPLAN is 100 kW, the operating efficiency $\eta ch,i$ and $\eta dis,i$ are taken as 0.9, and the maximum capacity is 600 kWh; the maximum capacity of the hydrogen storage is 150 kg, and the external tariffs of the grid use time-of-day tariffs as shown in Fig. 2.

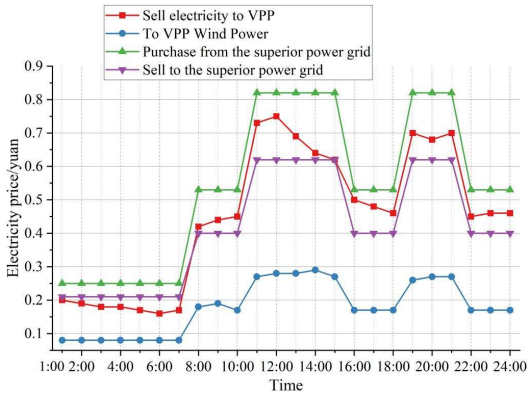

Figure 2: Time-of-use electricity purchase and sale prices

It can be seen that the price of electricity sold to VPP fluctuates from moment to moment, while the price of electricity purchased/sold to the higher-level grid is stable most of the time, as detailed analysis below. As far as the purchase of electricity from the higher power grid is concerned, the electricity price is 0.25 yuan from 1:00 to 7:00, 0.53 yuan per kWh from 8:00 to 10:00, 0.82 yuan per kWh from 11:00 to 15:00, 0.53 yuan per kWh from 16:00 to 18:00, 0.82 yuan per kWh from 19:00 to 21:00, and 0.53 yuan per kWh from 22:00 to 24:00. In the same way, the time fluctuation of electricity sales to the higher-level grid is the same as that of power purchase, but the electricity price is slightly lower, and the price of electricity is stable at "0.21, 0.4, 0.62, 0.4, 0.62, 0.4" in each period.

III. B. Optimization results

Based on the microgrid parameter design and EnergyPLAN model building shown in Table 1, this section adopts the improved snake optimization algorithm and CPLEX solver to carry out hierarchical optimization, and finally gives the scheduling results of microgrids A and B and the power trading strategy, revealing the facilitating effect of the low-carbon tariff mechanism on the flow of power in the system.

By modeling the microgrid, the multi-objective optimal scheduling results of the lower microgrid are given, and the optimal time-sharing tariffs of microgrid A and microgrid B are given after iterative coordination through system optimization as shown in Figs. 3 and 4.

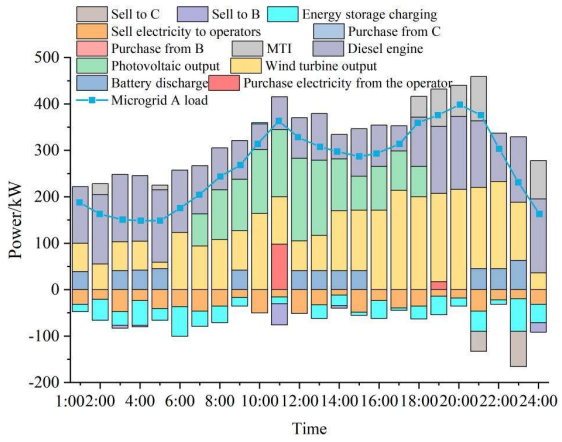

Figure 3: Microgrid A optimal dispatching

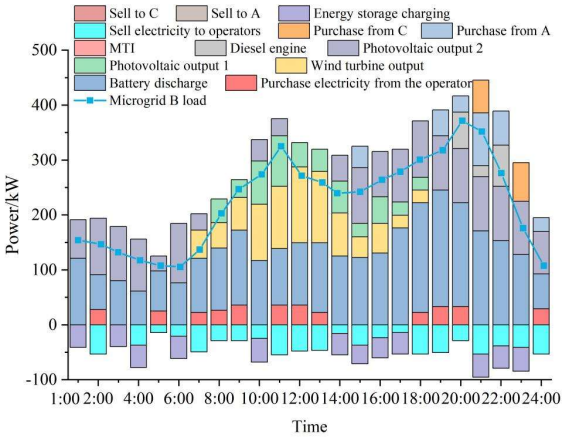

Figure 4: Microgrid B optimal dispatching

It can be clearly seen in the figure that at different moments, the microgrid, through its own various energy output, circulates electricity with other microgrids, and conducts power purchase and sale transactions with the microgrid group, and finally realizes that each microgrid can satisfy its own power load. It can be seen that the price of electricity inside the microgrid and EnergyPLAN is always smaller than the price of electricity outside the EnergyPLAN and the higher-level grid, which promotes the circulation of electricity in the EnergyPLAN system.

IV. Optimization of low-carbon transition path of power system

Through the validation of multi-objective optimization of the microgrid system, this chapter further extends the research scale to the power system as a whole, combining the sensitivity analysis of power generation cost, carbon emission and key parameters under different risk scenarios, and proposing a transition path planning strategy that takes into account the economic and low-carbon objectives.

IV. A. Power generation costs and carbon emissions

IV. A. 1) Power generation costs

Figures 5, 6, and 7 show the cost of each generation over the planning period for the generation portfolio for the low-risk, medium-risk, and high-risk scenarios, respectively.

The lowest total generation cost of 47.68 trillion yuan can be found for the planning period under the low-risk scenario. Of these, investment and construction costs account for the most significant portion of expenditures, about 28.93% of the total costs. Similarly, in the medium and high risk scenarios, investment and construction is also the most significant cost component, accounting for about 39.20% and 49.51% of the total cost, respectively. This is

mainly due to the fact that the medium and high risk scenarios require the construction of more renewable energy generating units compared to the low risk scenario to ensure the adequacy of power supply. It is worth noting that investment in generating units for China's power system is mainly concentrated in the 2020-2035 period. This further illustrates the need for China to complete its investment in renewable energy power plants as early as possible before 2035 and to bring them on line earlier to increase its fault tolerance for uncertain risks in the future. At the end of the planning horizon, the Low Risk Scenario requires the construction of more CCS equipment to reduce carbon emissions, as gas-fired generation still accounts for a larger share of electricity generation in the Low Risk Scenario. The cost of CCS in the Low Risk Scenario is as high as 534 million yuan, which is about 400 million yuan higher than the cost of CCS in the Medium and High Risk Scenarios. With the decrease in fuel prices, the fuel cost of the power generation mix gradually tends to decline. At the end of the planning stage, for the power generation combinations in low, medium and high-risk scenarios, their fuel costs were reduced from 1.5 billion yuan in the initial stage to 290 million yuan, 120 million yuan and 71 million yuan respectively. From the perspective of the numerical value of carbon cost, high-risk scenarios achieve profitability earlier than low-risk scenarios, but the difference is not significant. This phenomenon can be traced back to two reasons: On the one hand, as the proportion of power generation from renewable energy gradually increases, the differences in carbon emissions among various risk scenarios are relatively small; On the other hand, the current carbon price in China is still relatively low. A carbon price of 30 yuan per ton is not sufficient to have a significant impact on the total cost. Although high-risk scenarios have a slight advantage in terms of carbon costs, the difference between them and low-risk scenarios is not obvious. At the end of the planning stage, the environmental costs in all scenarios remained at a relatively low level, and the impact on the environment and society was small.

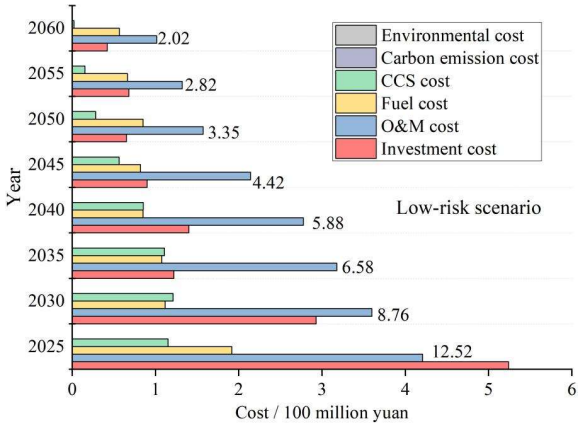

Figure 5: Power generation costs under low-risk scenarios

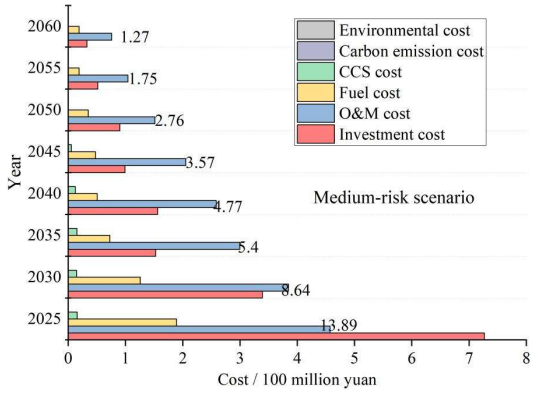

Figure 6: Power generation costs under medium-risk scenarios

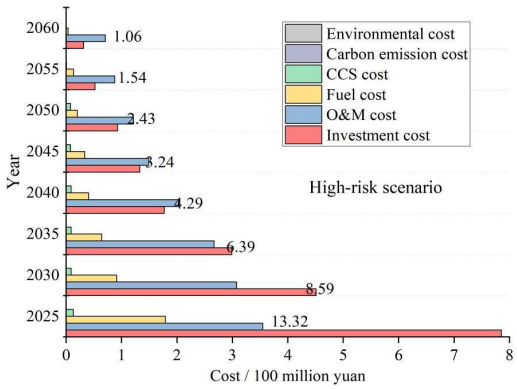

Figure 7: Power generation costs under high-risk scenarios

IV. A. 2) Carbon emissions

After clarifying the structural differences in the cost of power generation under different risk scenarios, this section further cuts through the dynamic changes in carbon emissions and analyzes the phase characteristics of the extreme emission reduction period, rapid emission reduction period and stable emission reduction period in the planning period, revealing the differential impacts of the proportion of renewable energy deployment and gas-fired power generation on the process of carbon neutrality.

The carbon emissions of the power generation mix under different risk scenarios are shown in Figure 8. In this paper, a total of eight planning phases are set up, and one planning phase covers five years, which is in line with the real development plan of China.

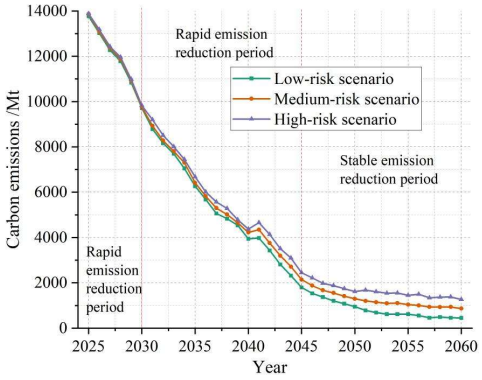

Figure 8: The carbon emissions under different risk scenarios

From the figure, it can be seen that the planning period can be divided into three stages according to the speed of carbon emission reduction, i.e., the extremely rapid emission reduction period, the rapid emission reduction period and the stable emission reduction period. Specifically, 2020-2030 is the period of extremely rapid emission reduction in China's power sector. During this period, the total carbon emissions are expected to be reduced by more than 4000 Mt, accounting for about 29.46% of the total emissions. The emission reduction effect and the percentage of emission reduction in this period reflect the Chinese government's determination and efforts to combat climate change and promote green energy transition. Between 2030 and 2045, China's power system will enter a period of rapid emission reduction. It is expected that by 2045, according to different risk scenarios, the total carbon emissions in this period will be about 1793.55Mt, 2142.21Mt and 2444.33Mt, with an average annual emission reduction of 522.64Mt, 570.28Mt and 648.84Mt, respectively.The emission reduction effect in this period is relatively significant, and the rate of emission reduction is slightly lower than that of the previous period of rapid emission reduction, but it still has a high emission reduction. However, it still has high emission reduction. The emission reduction targets for this period imply that the pressure on the power system to reduce emissions is still quite high, and the application of carbon emission reduction technologies and policy measures need to be further strengthened. During the period 2045-2060, China's power system enters a phase of stabilized emission reduction, with a relatively slowing down trend in the annual emission reduction rate. By the end of the planning period, there is little difference in total carbon emissions between the high-, medium- and low-risk scenarios, but the rate of

emission reduction is faster in the high-risk scenario. This phenomenon can be attributed to the fact that the high-risk scenario favors more renewable power generation, while gas-fired power generation in the low-risk scenario still occupies a certain share at the end of the planning period. During the stabilization period, China's power system should continue its efforts to promote the development and application of renewable energy in order to achieve a cleaner and low-carbon energy mix. At the same time, gas-fired power generation, as a relatively cleaner form of energy, will still maintain a certain share within a certain range. Taken together, the goal of the stabilization and emissions reduction period is to balance the use of various forms of energy in order to achieve sustainable development while safeguarding the stability of the electricity supply.

IV. B. Sensitivity analysis

The low-carbon transition pathway for the power system is influenced by a combination of technological, cost, and a variety of other factors, and is a complex system that is constantly evolving and changing dynamically. In order to provide a comprehensive assessment of low-carbon transition options, we have selected the following two key assumptions for sensitivity analysis, namely carbon pricing and energy storage share. Through the sensitivity analysis of these key factors, we can more accurately assess and optimize the low-carbon transition pathway of the power system, and provide decision makers with references and guidance with practical significance.

IV. B. 1) Carbon pricing

Figure 9 presents the level of carbon pricing over the planning period for different initial values of the carbon price, and Figure 10 illustrates the impact of different carbon price levels on the carbon emissions and generation costs of the generation portfolio under the low, medium and high risk scenarios.

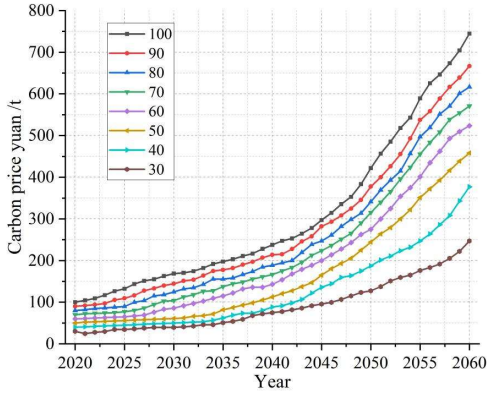

Figure 9: Carbon pricing levels with different initial values of carbon prices

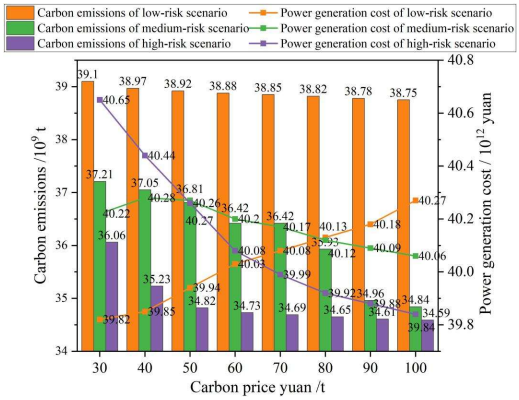

Figure 10: The impact on carbon emissions and power generation costs

It can be observed from the figure that a high carbon price can effectively reduce the carbon emissions of the power generation portfolio, which in turn promotes the process of carbon neutrality. Compared to the carbon price level with an initial value of 30 Yuan/tonne, the low, medium and high risk scenarios achieve carbon emission reductions of 0.35 billion tons, 237 million tons and 147 million tons, respectively, at a carbon price level with an initial value of 100 Yuan/tonne. This further indicates that the medium-risk scenario has the highest sensitivity to the

carbon price, while the low-risk scenario has the lowest sensitivity to the carbon price. To ensure the safety and reliability of the power system, it is necessary to maintain a fossil energy generation share of about 15% under the Low Risk Scenario even at the end of the planning horizon. In the medium and high risk scenarios, a reliable supply of electricity is ensured by increasing the installed capacity of renewable energy. In addition, the medium-risk scenario has the potential to deploy CCS equipment on a larger scale than the high-risk scenario in order to reduce the carbon emissions of the system without increasing the overall risk level.

The impact of the carbon price on the cost of electricity generation also varies across risk scenarios. As the carbon price level increases, the total cost of power generation for the medium and high risk scenarios shows a significant decreasing trend, while the cost of power generation for the low risk scenario increases. Based on a carbon price level with an initial value of 30 yuan per ton, the total costs of the medium and high-risk scenarios decrease by 0.16 trillion yuan and 0.81 trillion yuan, respectively, at a carbon price level with an initial value of 100 yuan per ton, which is mainly attributed to the benefits of increased carbon market revenues. However, the total cost of electricity generation in the low-risk scenario increases by 0.45 trillion yuan. On the one hand, this phenomenon stems from the increase in carbon price and the decrease in free allowances, resulting in thermal power companies in the low-risk scenario having to pay more for carbon allowances. On the other hand, due to the increase in carbon price, policy makers need to invest in more CCS units at the planning stage in order to reduce the overall carbon emissions of the power generation portfolio. In summary, the carbon pricing mechanism will play an important role in the carbon-neutral transition process, and can effectively reduce the carbon emissions of the power generation portfolio and the economic costs of renewable energy generation deployment, while at the same time significantly contributing to the promotion of low-carbon development and sustainable energy transition. However, the current level of carbon pricing in China is on the low side, and a high-level carbon pricing policy should be implemented as soon as possible in order to facilitate the low-carbon transition.

IV. B. 2) Share of energy storage

In order to assess the perturbation effects of key external factors on the transition path, this section further explores the impacts of changes in the share of energy storage on the unit cost of electricity generation and carbon emissions on the basis of the sensitivity analysis of carbon pricing, and proposes the optimization direction of replacing high-carbon units through energy storage technology.

Under different levels of energy storage share, the differences in unit carbon emissions and unit generation costs under low, medium and high risk scenarios are shown in Figure 11.

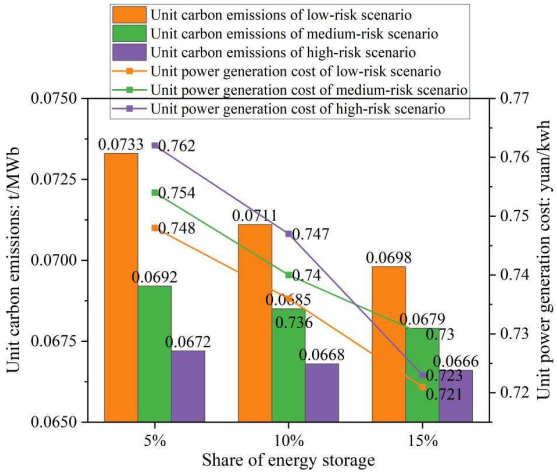

Figure 11: The differences in unit carbon emissions and power generation costs

As can be seen from the figure, a higher energy storage share has a significant impact on reducing the unit generation cost of the generation portfolio. Specifically, increasing the share of energy storage from 5% to 15% reduces the unit generation cost of the generation portfolio by 0.027 yuan/kWh, 0.024 yuan/kWh, and 0.039 yuan/kWh in the low-risk, medium-risk, and high-risk scenarios, respectively, which saves policymakers about 1.51 trillion, 1.28 trillion, and 2.07 trillion yuan, respectively. Increasing the share of energy storage is most effective in reducing costs in the high-risk scenario, but less effective in reducing unit carbon emissions, which are reduced by only 0.005 tons/MWh. This may be due to the fact that unit carbon emissions from the generation portfolio are inherently relatively low in the high-risk scenario and that the cost of energy storage technologies is significantly

lower than the cost of some of the renewable generation equipment. As a result, policymakers are more inclined to reduce the investment and O&M costs of renewable energy equipment by increasing the proportion of energy storage in the generation mix. With a lower level of risk and no carbon emission pitfalls compared to other generation technologies, energy storage can be an important technology for power balancing and peaking. Accordingly, policymakers can reduce carbon emissions from the power generation mix by increasing investment in energy storage equipment to replace fossil energy generating units with higher carbon emissions. Specifically, when the share of energy storage is increased from 5% to 15%, the low-risk scenario has the largest reduction in carbon emissions per unit of the generation portfolio, reaching 0.027 tons/MWh, a reduction of 148 million tons of carbon emissions. It is worth noting that as energy storage technology continues to advance, its cost will be further reduced, which will also further lower the unit cost of electricity generation for the generation portfolio.

V. Conclusion

Through multi-scale modeling and multi-objective optimization, this paper systematically analyzes the key paths of power structure transformation under the dual-carbon target, and the main conclusions are as follows.

The incentive-based demand response model based on nodal carbon potential significantly optimizes the spatial and temporal distribution of loads, reduces the dispatch cost of transferable loads by 21%, and improves the rate of wind and solar energy consumption to 89.2%; and the stepped carbon trading model promotes the increase of carbon emissions trading volume by 34% through the price growth coefficient to strengthen the initiative of users to reduce carbon emissions.

Under the high-risk scenario, the proportion of renewable energy installed capacity needs to reach 65% by 2035, combined with a 15% share of energy storage can reduce the unit cost of power generation to 0.102 yuan/kWh, which is 42% less than the cost of the traditional thermal power-led model. Gas-fired power generation retains a 15% share and is supported by CCS technology (at a cost of 534 million yuan), which balances system stability and emission reduction targets.

The carbon price level has the most significant impact on the medium-risk scenario, with a 5.2Mt increase in average annual emissions reduction for every 10RMB/ton increase in the carbon price; a 10% decrease in the cost of energy storage technology reduces unit carbon emissions by 0.008 tons/MWh.

References

[1] Nogrady, B. (2021). China launches world's biggest carbon market. Nature, 595(637), 1.

[2] Hepburn, C., Qi, Y., Stern, N., Ward, B., Xie, C., & Zenghelis, D. (2021). Towards carbon neutrality and China's 14th Five-Year Plan: Clean energy transition, sustainable urban development, and investment priorities. Environmental Science and Ecotechnology, 8, 100130.

[3] Tang, B., Li, R., Yu, B., An, R., & Wei, Y. M. (2018). How to peak carbon emissions in China's power sector: a regional perspective. Energy Policy, 120, 365-381.

[4] Ma, X., Wang, C., Dong, B., Gu, G., Chen, R., Li, Y., ... & Li, Q. (2019). Carbon emissions from energy consumption in China: Its measurement and driving factors. Science of the total environment, 648, 1411-1420.

[5] Li, Y., Niu, D., & Song, J. (2022). Decoupling analysis of carbon emissions in China's power industry—based on ARDL model. Environmental Science and Pollution Research, 29(37), 56535-56554.

[6] Mohsin, M., Hanif, I., Taghizadeh-Hesary, F., Abbas, Q., & Iqbal, W. (2021). Nexus between energy efficiency and electricity reforms: a DEA-based way forward for clean power development. Energy Policy, 149, 112052.

[7] Guang, F., & Wen, L. (2020). Growth pattern changes in China's energy consumption. Environmental Science and Pollution Research, 27(22), 28360-28373.

[8] Hao, J., Chen, L., & Zhang, N. (2022). A statistical review of considerations on the implementation path of China's "double carbon" goal. Sustainability, 14(18), 11274.

[9] Wang, Y., Zhang, Q., & Li, C. (2019). The contribution of non-fossil power generation to reduction of electricity-related CO2 emissions: a panel quintile regression analysis. Journal of Cleaner Production, 207, 531-541.

[10] Wang, W., Yu, T., Huang, Y., Han, Y., Liu, D., & Shen, Y. (2021). The situation and suggestions of the new energy power system under the background of carbon reduction in China. Energy Reports, 7, 1477-1484.

[11] Liu, Y., & Duan, C. (2023, April). Analysis of China's power system transformation. In IOP Conference Series: Earth and Environmental Science (Vol. 1171, No. 1, p. 012009). IOP Publishing.

[12] Dong, J., Liu, D., Dou, X., Li, B., Lv, S., Jiang, Y., & Ma, T. (2021). Key issues and technical applications in the study of power markets as the system adapts to the new power system in China. Sustainability, 13(23), 13409.

[13] Feng, T. T., Yang, Y. S., & Yang, Y. H. (2018). What will happen to the power supply structure and CO2 emissions reduction when TGC meets CET in the electricity market in China?. Renewable and Sustainable Energy Reviews, 92, 121-132.

[14] Qin, B., Wang, M., Zhang, G., & Zhang, Z. (2022). Impact of renewable energy penetration rate on power system frequency stability. Energy Reports, 8, 997-1003.

[15] Wang, D., Zhang, S., Wang, Y., & Mao, J. (2022). Impact of spatial misallocation of electric power resources on economic efficiency and carbon emissions in China. Environmental Science and Pollution Research, 29(36), 55250-55277.

[16] Silva, B. N., Khan, M., & Han, K. (2020). Futuristic sustainable energy management in smart environments: A review of peak load shaving and demand response strategies, challenges, and opportunities. Sustainability, 12(14), 5561.

[17] Alsagri, A. S., & Alrobaian, A. A. (2022). Optimization of combined heat and power systems by meta-heuristic algorithms: An overview. Energies, 15(16), 5977.